Fabrication of a novel lumped electro-absorption modulator with a lower RC-time constant*

Qiu Yingping(邱应平)†, Wang Yang(汪洋), Shao Yongbo(邵永波), Zhou Daibing(周代兵), Liang Song(梁松), Zhao Lingjuan(赵玲娟), and Wang Wei(王圩)

Key Laboratory of Semiconductor Materials Science, Institute of Semiconductors, Chinese Academy of Sciences, Beijing 100083, China

Abstract: A novel lumped electro-absorption modulator with a charge layer and an undercut ridge waveguide (DU-EAM) was fabricated and measured. Also, two other kinds of EAM with straight ridge waveguides, one with a charge layer (D-EAM) and another with no charge layer (N-EAM), were fabricated and tested to ensure that the design of the DU-EAM would reduce the RC-time constant. The measured capacitance of the D-EAM and the DU-EAM is lower than that of the N-EAM under reverse bias voltage from –1 to –8 V due to the inserted charge layer. The capacitances of the N-EAM, the D-EAM and the DU-EAM are 0.375, 0.225 and 0.325 pF, respectively, at –3 V. In addition, the DU-EAM had a larger extinction ratio (25 dB at –3 V) and higher modulation efficiency (13 dB/V between –1 and –2 V) than two other straight-ridge-waveguide ones (the D-EAM performed 22 dB and 10 dB/V, the N-EAM performed 20 dB and 10 dB/V) due to the 5.2 μm wider active region.

Key words: undercut waveguide; charge layer; modulation efficiency dual-depletion; capacitance; extinction ratio
DOI: 10.1088/1674-4926/32/10/105002 **EEACC:** 4250; 4150

1. Introduction

With the overwhelming growth of Internet access and personal communication systems (PCS), wider bandwidth and higher efficiency semiconductor electro-absorption modulators (EAMs) based on the quantum-confined Stark effect[1] of a multiple quantum well (MQW) structure are attractive modulation devices for both analog and digital fiber optic links due to their compact size, high modulation efficiency and potential to integrate with other components. A lumped EAM with a straight ridge waveguide has been widely researched because of its simple fabrication process. However, the 3-dB bandwidth of an usual lumped EAM cannot satisfy the need for high bit rates of the rapid communication system development due to the limitation of the RC-time constant[2, 3].

Theory and experiment have proved that an inserted 50-nm n-InP (5×10^{18}) and a 400-nm i-InGaAsP collection layer between the active layer and the buffer layer of an EAM could serve as a charge layer and a exhaustion region that would concentrate almost all of the external applied electric field in the MQW region. In this work, a novel DU-EAM with a charge layer[4–6] and an undercut ridge waveguide[7–9] was proposed. A novel undercut ridge waveguide, composed of an undercut layer and a straight layer, was designed to increase w ($R = \rho\frac{l}{Aw}$) to reduce the series resistance R of the DU-EAM. In addition, two other kinds of EAM, such as N-EAM and D-EAM, were fabricated as the compared structure devices. The capacitance and static extinction ratio of the three kinds of device were measured and analyzed. The measured results demonstrated that the D-EAM and the DU-EAM did perform at lower capacitance than the N-EAM and the DU-EAM with a 5.2 μm wider active region and had a larger ER than that of two other kinds of device.

2. Device design and fabrication

Here, the three types of EAMs with different structures were designed and fabricated as follows.

The materials for the three devices were grown by Aixtron AG 200 MOCVD, as shown in Table 1. The multiple quantum well active region of all of the devices were composed of 8 tensile strained wells (1504-nm-InGaAsP) and 8 compressed strained barriers (1.2Q-InGaAsP). In the devices of the D-EAM and the DU-EAM, a 50-nm n-InP (5×10^{18}) charge layer and a 400-nm i-InGaAsP (1.2Q) collection layer were sandwiched between the lower confined layer and the buffer layer. The applied electric field was be almost concentrated on the 8QW active layer and the capacitance including the junction capacitance and the parasitic capacitance was successfully reduced.

Figure 1 shows the photoluminescence spectra of InGaAsP 8QW, which is satisfied as the active layer of a 1550 nm EA modulator.

Then, a novel etching method with two steps, including chemical wet etching followed by RIE dry etching[10], was proposed to get an undercut-ridge waveguide, the SEM picture of which is shown in Fig. 2. Both the N-EAM and the D-EAM have 2.5 μm single-straight waveguides. The undercut ridge waveguide with a 5.2 μm wide upper table-board and a 3.5 μm narrow lower table-board in the DU-EAM means a 5.2 μm wider 8QW active region. All of the devices were polarized by polyimide after the ridge etching process and silicon diox-

* Project supported by the State Key Development Program for Basic Research of China (No. 2011CB301702).
† Corresponding author. Email: ypqiu@semi.ac.cn
Received 13 April 2011, revised manuscript received 4 May 2011

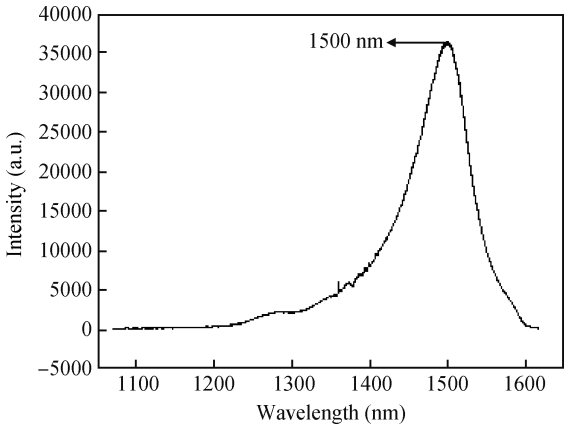

Fig. 1. Measured photoluminescence spectrum of InGaAsP 8QW.

Table 1. Structures of the N-EAM, D-EAM and DU-EAM.

	Material	Waveguide
N-EAM	Contact layer p-InGaAs Cladding layer p-InP Confined layer i-InGaAsP (1.2Q) 8QW i-InGaAsP (1.5Q) Confined layer i-InGaAsP (1.2Q) Buffer layer n-InP Substrate n-InP	Straight-ridge waveguide
D-EAM	Contact layer p-InGaAs Cladding layer p-InP Confined layer i-InGaAsP (1.2Q) 8QW i-InGaAsP (1.5Q) Confined layer i-InGaAsP (1.2Q) Charge layer n-InP (5E18) Collection layer i-InGaAsP (1.2Q) Buffer layer n-InP Substrate n-InP	Straight-ridge waveguide
DU-EAM	Contact layer p-InGaAs Cladding layer p-InP Confined layer i-InGaAsP (1.2Q) 8QW i-InGaAsP (1.5Q) Confined layer i-InGaAsP (1.2Q) Charge layer n-InP (5E18) Collection layer i-InGaAsP (1.2Q) Buffer layer n-InP Substrate n-InP	Undercut-ridge waveguide

ide deposition to get a flat surface for electrode fabrication and to lower the parasite capacitance. Figure 3 shows a top view of the devices.

3. Results and discussion

As is well known, the 3-dB bandwidth of the lumped EAM is mainly determined by the resistance–capacitance (RC) time constant. A low capacitance is the key factor of a large 3-dB

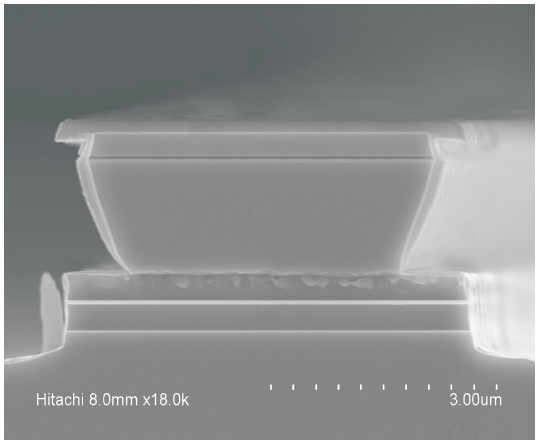

Fig. 2. Structure of undercut ridge waveguide.

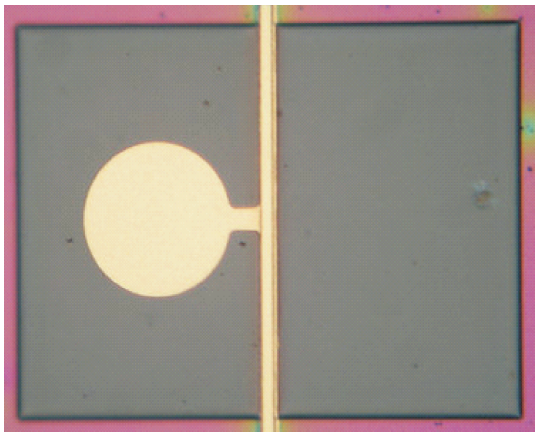

Fig. 3. Picture of a real EAM device and an undercut ridge waveguide.

bandwidth of lumped EAM. To enable high speed modulation, the D-EAM and the DU-EAM with lower capacitance structure were designed and fabricated. The static capacitance of the devices with a length of 250 μm was measured under reverse bias voltage from –1 to –8 V by using an HP4275A MUTI-FREQUENCY LCR METER at 1MHz and that of the N-EAM (a no charge layer EAM) was also measured for comparison with them, as shown in Fig. 4.

Compared with the capacitance of the N-EAM, the D-EAM has the lowest capacitance of 0.225 pF at –3 V. Considering $f_{3\mathrm{dB}} = \frac{1}{\pi R_{\mathrm{eff}} C_{\mathrm{J}}}$ and $R_{\mathrm{eff}} = 50\ \Omega$, the 3-dB bandwidth of 28.3 GHz of the DU-EAM could be achieved at an optimal bias voltage of –3 V. The results indicate that an inserted charge layer in the D-EAM resulted in a decrease in capacitance and a corresponding increase of 3 dB bandwidth. On the other hand, it can be seen from Fig. 4 that the DU-EAM has a larger capacitance of 0.325 pF than 0.225 pF of D-EAM at –3 V due to the 3 μm upper capacitor plate (p-InP) and the 5 μm wider lower capacitor plate compared with the 3 μm straight ridge waveguide in the N-EAM. The corresponding $f_{3\mathrm{dB}}$ of the DU-EAM and the N-EAM are 19.6 GHz and 16.9 GHz.

Another important parameter of an EAM we focus on is the static DC extinction ratio (ER) at 1550 nm under reverse bias voltage, which is mainly determined by the cavity length and the active region width of devices. The measured results

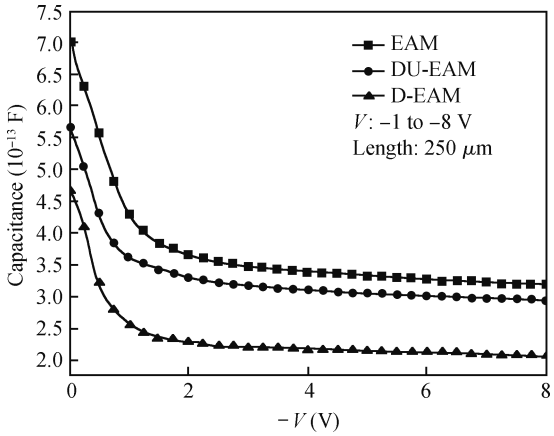

Fig. 4. Measured capacitance of three types of EAM with a length of 250 μm.

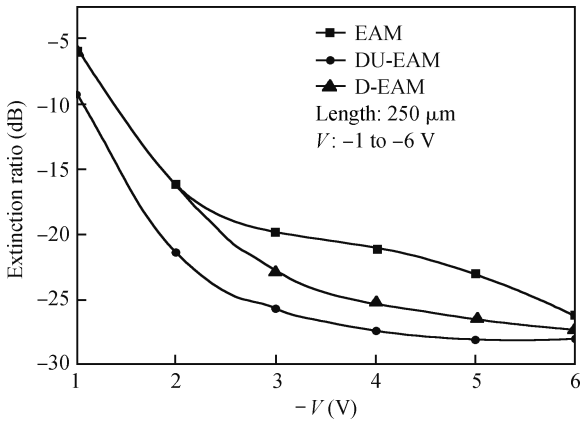

Fig. 5. Measured extinction ratio of three types of EAM with a length of 250 μm at 1550 nm under reverse bias voltage from –1 to –6 V.

of the ER of the devices with a 250-μm-long waveguide under DC reverse bias voltage from –1 to –6 V is shown in Fig. 5. As can be seen from the diagram, the ER of the DU-EAM is about 25 dB at –3 V and the modulation efficiency is about 13 dB/V between –1 and –2 V, both of which are larger than that of the N-EAM and the D-EAM. This may be result from the 5 nm wider active region. The ER of the N-EAM and the D-EAM is 20 dB and 22 dB at –3 V and the modulation efficiency of the N-EAM and the D-EAM is 10 dB/V and 10 dB/V between –1 and –2 V.

The small differences in ER between the N-EAM and the D-EAM might be explained by the hypothesis that the inserted charge layer and collection layer would narrow the exhaustion region to strengthen the applied electric field in the 8QW region[11, 12].

In addition, to figure out the effect of cavity length on the ER, the static extinction ratio of the DU-EAM with different cavity lengths was measured, as shown in Fig. 6. The DU-EAM with the greatest length of 250 μm has the largest ER of about 25 dB at –3 V and the highest modulation efficiency of about 13 dB/V between –1 and –2 V. Correspondingly, the ER and modulation efficiency of the shortest DU-EAM with a length of 120 μm is 12 dB at –3 V and 6 dB/V between –1 and –2 V. All of the above results show that the ER and modulation efficiency

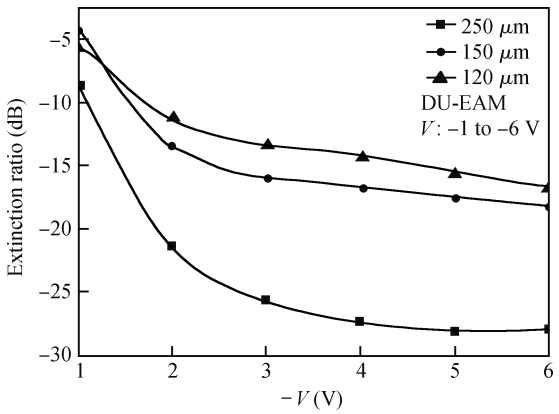

Fig. 6. Measured extinction ratio of the DU-EAM with different cavity lengths at 1550 nm under reverse bias voltage from –1 to –6 V.

of the lumped devices would accrete with the increased cavity length.

4. Conclusion

In summary, the three kinds of lumped EAMs, including the N-EAM, the D-EAM and the DU-EAM, were successfully fabricated. The 3-dB bandwidth of the D-EAM with a length of 250 μm can achieve the highest of 28.3 GHz at –3 V. A DU-EAM with an undercut ridge waveguide, composed of a 4 μm wide upper table-board and a 2 μm narrow lower table-board, may be fabricated in future work to improve the f_{3dB}. In addition, as high as 25 dB (at –3 V) and 13 dB/V (–1 to –2 V) of the DU-EAM with a length of 250 μm were attained. Even the ER and modulation efficiency of the DU-EAM with a length of 120 μm achieved 12 dB at –3 V and 6 dB/V between –1 and –2 V.

Acknowledgements

The authors would like to thank Niu Bin and Bian Jing for help with measurement and also Wang Baojun for help with fabrication.

References

[1] Irmscher S. Design, fabrication and analysis of InP-InGaAsP traveling-wave electro-absorption modulators. Doctoral Thesis, KTH, 2003
[2] Li G L, Sun C K, Pappert S A, et al. Ultrahigh-speed traveling-wave electroabsorption modulator design and analysis. IEEE Trans Microw Theory Tech, 1999, 47(7): 1177
[3] Li G L. Wide bandwidth high efficiency electro-absorption modulators for analog fiber-optic links. PhD Dissertation, UCSD, 2002
[4] Shi J W, Hsieh C A, Shiao A C, et al. Demonstration of a dual-depletion-region electroabsorption modulator at 1.55 μm wavelength for high-speed and low-driving-voltage performance. IEEE Photonics Technol Lett, 2005, 17(10): 2068
[5] Shi J W, ShiaoA C. A dual depletion region electroabsorption modulator at 1.55 μm wavelength for high speed and low driving voltage performance. IEEE OWC3, 2005
[6] Anselm K A, Nie H, Hu C, et al. Performance of thin separate absorption, charge and multiplication avalanche photodiodes. IEEE

J Quantum Electron, 1998, 34(3): 482
[7] Pasquariello D, Bjorlin E S, Lasaosa D, et al. Selective undercut etching of InGaAs and InGaAsP quantum wells of improved performance of long-wavelength optoelectronic devices. J Lightwave Technol, 2006, 24(3): 1470
[8] Wu T H, Chiu Y J, Lin F Z. High-speed (60 GHz) and low-voltage-driving electroabsorption modulator using two-consecutive-steps selective-undercut-wet-etching waveguide. IEEE Photonics Technol Lett, 2008, 20(14): 1261
[9] Dummer M M, Raring J R, Klamkin J, et al. Selective-undercut traveling-wave electro-absorption modulators incorporating a p-InGaAs contact layer. Opt Express, 2008, 16(25): 20388
[10] Arrioja D A M. Integrated InP photonic switches. Graduated Thesis, Central Florida, 2002
[11] Nie H, Anselm K A, Lenox C, et al. Resonant cavity separate absorption, charge and multiplication avalanche photodiodes with high speed and high gain-bandwidth product. IEEE Photonics Technol Lett, 1998, 10(3): 409
[12] Dries J C, Thomson K J, Forrest S R. $In_{0.53}Ga_{0.47}As/In_{0.52}Al_{0.48}As$ separate absorption, charge, and multiplication layer long wavelength avalanche photodiode. Electron Lett, 1999, 35(4): 334